

# High-Temperature Behavior of CsH<sub>2</sub>PO<sub>4</sub> under Both Ambient and High Pressure Conditions

Dane A. Boysen and Sossina M. Haile\*

Keck Laboratories, Department of Materials Science 138-78, California Institute of Technology,  
Pasadena, California 91125

Hongjian Liu and Richard A. Secco

Department of Earth Sciences, University of Western Ontario,  
London, Ontario, N6A 5B7, Canada

Received October 4, 2002

The high-temperature behavior of CsH<sub>2</sub>PO<sub>4</sub> has been carefully examined under both ambient and high pressure (1.0 ± 0.2 GPa) conditions. Ambient pressure experiments encompassed thermal analysis, AC impedance spectroscopy, <sup>1</sup>H NMR spectroscopy, and polarized light microscopy. Simultaneous thermogravimetric analysis, differential scanning calorimetry, and evolved gas analysis by mass spectroscopy demonstrated that a structural transition with an enthalpy of 49.0 ± 2.5 J/g occurred at 228 ± 2 °C, just prior to thermal decomposition. The details of the decomposition pathway were highly dependent on sample surface area, however the structural transformation, a superprotonic transition, was not. Polarized light microscopy showed the high temperature phase to be optically isotropic in nature, consistent with earlier suggestions that this phase is cubic. The conductivity of CsH<sub>2</sub>PO<sub>4</sub>, as revealed by the impedance measurements, exhibited a sharp increase at the transition temperature, from 1.2 × 10<sup>-5</sup> to 9.0 × 10<sup>-3</sup> Ω<sup>-1</sup>cm<sup>-1</sup>, followed by a rapid decline due to dehydration. In addition, chemically adsorbed surface water was shown to increase the conductivity of polycrystalline CsH<sub>2</sub>PO<sub>4</sub> over well-dried samples, even at mildly elevated temperatures (>200 °C). At high pressure an apparent irreversible phase transition at 150 °C and a reversible superprotonic phase transition at 260 °C were observed by impedance spectroscopy. At the superprotonic transition, the conductivity increased sharply by ~3 orders of magnitude to 3.5 × 10<sup>-2</sup> Ω<sup>-1</sup>cm<sup>-1</sup> at 275 °C. This high conductivity phase was stable to the highest temperature examined, 375 °C, and exhibited reproducible and highly Arrhenius conduction behavior, with an activation energy for charge transport of 0.35 eV. Upon cooling, CsH<sub>2</sub>PO<sub>4</sub> remained in the high-temperature phase to a temperature of 240 °C.

## Introduction

Cesium dihydrogen phosphate, CsH<sub>2</sub>PO<sub>4</sub>, has received attention because of both its high-temperature proton transport properties and its low-temperature ferroelectric properties. Although there is wide agreement on the low-temperature behavior of this material — that it undergoes a ferroelectric phase transition at 154 K (*P*<sub>2<sub>1</sub>/m → *P*<sub>2<sub>1</sub>)<sup>1,2</sup> — there is significant discrepancy in the literature regarding its high-temperature properties. It has been observed that, upon heating, the conductivity of CsH<sub>2</sub>PO<sub>4</sub> undergoes a sharp increase at 230 °C.<sup>3–5</sup> Some, including Baranov et al.,<sup>3</sup> Romain and Novak,<sup>6</sup> Preisinger et al.,<sup>7</sup> and Luspín et al.,<sup>8</sup> attribute this</sub></sub>

behavior to a structural transition to a stable, high-temperature phase (a so-called superprotonic transition), whereas others, including Lee<sup>9</sup> and Ortiz et al.,<sup>5</sup> attribute the increase in conductivity to an artifact of water loss due to thermal decomposition.

Whether or not CsH<sub>2</sub>PO<sub>4</sub> undergoes a superprotonic transition is of particular relevance to understanding the role of hydrogen bonding in structural phase transformations. Under ambient temperature and pressure conditions, this compound has a unique hydrogen bond network in which PO<sub>4</sub><sup>3-</sup> anions are linked via O–H···O bonds at all corners of the phosphate tetrahedra, forming [H<sub>2</sub>(PO<sub>4</sub>)<sup>-</sup>]<sub>∞</sub> layers. Cesium cations reside at sites between these layers. Plakida<sup>10</sup> has treated the superprotonic phase transition in the related compound, CsHSO<sub>4</sub>, in terms of a microscopic model that assumes an order–disorder relationship between the low- and high-temperature phases. Although not stated explicitly,

\* Corresponding author. Phone (626) 395-3958. Fax (626) 395-3933. E-mail: smhaile@caltech.edu.

(1) Levstik, A.; Blinc, R.; Kadaba, P.; Cizikov, S.; Levstik, I.; Filipic, C. *Solid State Commun.* **1975**, *16*, 1339.

(2) Uesu, Y.; Kobayashi, J. *Phys. Status Solidi A* **1976**, *34*, 475.

(3) Baranov, A. I.; Khiznichenko, V. P.; Shuvalov, L. A. *Ferroelectrics* **1989**, *100*, 135.

(4) Haile, S. M. *Mater. Res. Soc. Symp. Proc.* **1999**, *547*, 315.

(5) Ortiz, E.; Vargas, R. A.; Mellander, B.-E. *J. Chem. Phys.* **1999**, *110*, 4847.

(6) Romain, F.; Novak, A. *J. Mol. Struct.* **1991**, *263*, 69.

(7) Preisinger, A.; Mereiter, K.; Bronowska, W. *Mater. Sci. Forum* **1994**, *166–169*, 511.

(8) Luspín, Y.; Vaills, Y.; Hauret, G. *J. Phys. I* **1997**, *785*.

(9) Lee, K.-S. *J. Phys. Chem. Solids* **1996**, *57*, 333.

(10) Plakida, N. M. *Phys. Status Solidi B* **1986**, *135*, 133.

such a model rules out the possibility of a superprotonic transition in a compound such as  $\text{CsH}_2\text{PO}_4$ , in which all oxygen atoms participate in hydrogen bond formation. This observation had earlier led the present authors to suggest that a superprotonic phase is unlikely in  $\text{CsH}_2\text{PO}_4$ , while acknowledging that the experimental evidence remained inconclusive.<sup>4,11</sup>

Accordingly, the broad objective of the present study is to establish unequivocally whether  $\text{CsH}_2\text{PO}_4$  undergoes a transition to a high conductivity phase prior to decomposition. In the first portion of the study, the dehydration and phase-transition behavior, and the effect of surface water on conductivity at ambient pressures are presented. It is demonstrated that, even under ambient pressure conditions, a high-temperature phase transition occurs that is independent of decomposition. The short-lived nature of this phase, however, precludes accurate measurement of its electrical properties. To address this challenge, in the second portion, we employ high pressure during conductivity measurements, with the aim of suppressing dehydration and enabling complete characterization of the high-temperature phase. Before presenting the results of these sets of studies, we briefly summarize the prior state of knowledge regarding  $\text{CsH}_2\text{PO}_4$  at elevated temperatures.

### Background

As an example of the controversy surrounding the high-temperature behavior of  $\text{CsH}_2\text{PO}_4$ , the thermal gravimetric and differential thermal analysis (TGA and DTA) data reported by Rashkovich et al.,<sup>12</sup> Ortiz et al.,<sup>5</sup> and Nirsha et al.<sup>13</sup> are presented in Figure 1. It is immediately evident that there are significant discrepancies between these three sets of results. Rashkovich et al. have reported two structural (polymorphic) phase transitions, at 230 and at 256 °C (as quoted in the manuscript, however, the data indicate that the second transition is at 269 °C), prior to decomposition, the onset of which occurs at ~300 °C. Data were collected only for temperatures of 180 °C and higher. In a later paper, Rashkovich and Meteva<sup>14</sup> reported high-temperature diffraction data and proposed that the formation of an intermediate phase of "symmetry no higher than monoclinic" was responsible for the transition at 230 °C. In addition, they showed that the main peaks of  $\text{CsPO}_3$  appeared at temperatures as low as 100 °C, and that this phase was well-formed by 250 °C, although weight loss was not observed until higher temperatures were reached. Differential scanning calorimetry (DSC) measurements of Metcalfe and Clark<sup>15</sup> (not shown in Figure 1) indicate the presence of two polymorphic transitions, one at 149 °C (quasi-irreversible) and the latter at 230 °C (reversible), with decomposition occurring at temperatures above ~250 °C, in relatively good agreement with Rashkovich et al. for the temperature regime of mutual examination.

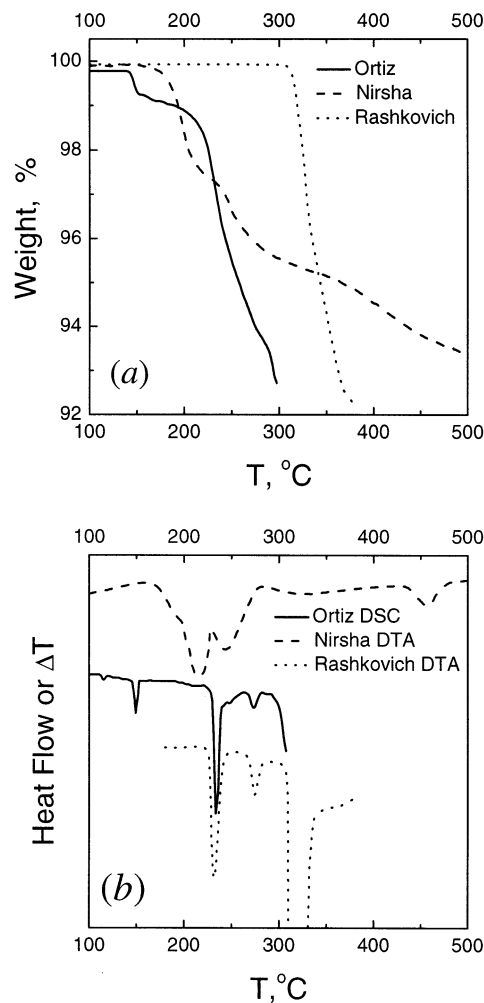


**Figure 1.** Prior thermal analysis results reported for  $\text{CsH}_2\text{PO}_4$  by Ortiz et al.,<sup>5</sup> Nirsha et al.,<sup>13</sup> and Rashkovich et al.:<sup>12</sup> (a) thermal gravimetry (TG) data, and (b) differential scanning calorimetry (DSC) and differential thermal analysis (DTA) data.

In contrast, Nirsha et al.<sup>13</sup> reported that thermal events occur at ~220 and 255 °C and are both due to thermal decomposition, with the compound  $\text{Cs}_2\text{H}_2\text{P}_2\text{O}_7$  forming over the temperature range 175–225 °C and  $\text{CsPO}_3$  forming over the range 235–285 °C. This interpretation was supported by high-temperature diffraction data and IR spectra. Thermal events evident in the DTA data at higher temperatures were ascribed to the crystallization of the initially amorphous  $\text{CsPO}_3$ . The conclusions drawn by Ortiz et al.<sup>5</sup> from their results are in general agreement with the findings of Nirsha et al. although they differ in detail. Quite surprisingly, the DSC data of Ortiz et al. match the DTA data of Rashkovich et al., but their TGA results differ significantly. Consistent with the results of Rashkovich et al., Ortiz and co-workers observe thermal events at ~149, 231, and 273 °C (the latter two also observed by Rashkovich), all of which coincide with peaks in their differential thermal analysis data. Accordingly, they ascribe all three, along with discontinuities in the conductivity of  $\text{CsH}_2\text{PO}_4$  (Figure 2) at 149 and 231 °C, to thermal dehydration and partial polymerization (i.e., polycondensation of phosphate groups).

A completely different interpretation of the high-temperature behavior of  $\text{CsH}_2\text{PO}_4$  has been offered by

(11) Haile, S. M.; Lentz, G.; Kreuer, K.-D.; Maier, J. *Solid State Ionics* **1995**, *77*, 128.

(12) Rashkovich, L. H.; Meteva, K. B.; Shevchik, Ya. E.; Hoffman, V. G.; Mishchenko, A. V. *Sov. Phys. Crystallogr.* **1977**, *22*, 613.

(13) Nirsha, B. M.; Gudimitsa, E. N.; Fakeev, A. A.; Efremov, V. A.; Zhadanov, B. V.; Olikova, V. A. *Russ. J. Inorg. Chem.* **1982**, *27*, 770.

(14) Rashkovich, L. N.; Meteva, K. B. *Sov. Phys. Crystallogr.* **1978**, *23*, 447.

(15) Metcalfe, B.; Clark, J. B. *Thermochim. Acta* **1978**, *24*, 149.

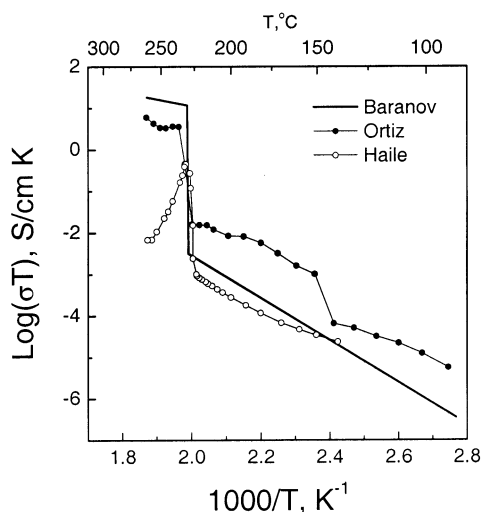


**Figure 2.** Prior conductivity data reported for  $\text{CsH}_2\text{PO}_4$  by Baranov et al.,<sup>3</sup> Ortiz et al.,<sup>5</sup> and Haile,<sup>4</sup> plotted in Arrhenius form.

a number of authors, specifically, that at  $\sim 230$  °C the material transforms to a phase of cubic symmetry with superprotonic conductivity. The conductivity of  $\text{CsH}_2\text{PO}_4$ , as reported by several authors, is reproduced in Figure 2.<sup>3,5</sup> It is evident that all authors are in agreement that the conductivity increases sharply at  $\sim 230$  °C, but only Baranov et al.<sup>3</sup> have attributed the increase to a transformation to a thermally stable, superprotonic phase. They report the activation energy for proton transport in this phase to be 0.32 eV, and the magnitude of the conductivity at 230 °C to be  $2.3 \times 10^{-2}$  S/cm, somewhat higher than others have observed. In contrast, Ortiz et al.<sup>5</sup> flatly ruled out the possibility of a polymorphic phase transformation, as described above. Haile<sup>4</sup> observed that the conductivity of  $\text{CsH}_2\text{PO}_4$  immediately decreased after the transition at 230 °C, and concluded that if a superprotonic phase did indeed exist, it was a highly transient state, immediately followed by decomposition. Prolonged examinations of the electrical properties of  $\text{CsH}_2\text{PO}_4$  by Ortiz et al.<sup>5</sup> showed a similar degradation in conductivity with time.

Very convincing data for the presence of a cubic, high-temperature phase of  $\text{CsH}_2\text{PO}_4$  has been presented by Preisinger et al.<sup>7</sup> (see also refs 16 and 17), who performed diffraction experiments at elevated temperatures. Under dry atmospheres, dehydration and the formation of  $\text{CsH}_2\text{P}_2\text{O}_7$  were observed, but under humidified conditions, a stable cubic phase ( $Pm\bar{3}m$ ,  $a = 4.961$  Å) appeared at temperatures above 230 °C. Baranov et al. had earlier proposed that their superprotonic phase was cubic on the basis of optical microscopy investigations, which showed the phase to be optically isotropic.<sup>3</sup> Further evidence for a polymorphic transition at 230 °C comes from the work of Romain and Novak,<sup>6</sup> who showed by high-temperature Raman spectroscopy that there is no evidence of  $\text{CsH}_2\text{P}_2\text{O}_7$  formation up to temperatures as high as 246 °C. Moreover, in a comprehensive study of the high-temperature, high-pressure behavior of  $\text{CsH}_2\text{PO}_4$ , Rapoport et al.<sup>18</sup>

observed a stable, high-temperature phase that transformed reversibly to and from the lower-temperature monoclinic form at elevated pressures.

In addition to the competing views as to whether the transition at 230 °C in  $\text{CsH}_2\text{PO}_4$  corresponds to decomposition or a polymorphic transition, there is significant discrepancy regarding the behavior in the temperature regime 100–150 °C. As noted above, Ortiz et al.<sup>5</sup> suggest that  $\text{CsH}_2\text{PO}_4$  undergoes a thermal decomposition event at a temperature of 149 °C which, much like the transition at 230 °C, gives rise to an increase in conductivity. Others have ascribed the transition at this temperature to a subtle, polymorphic, monoclinic  $\rightarrow$  monoclinic transformation. Evidence for this interpretation is provided by Bronowska and Pietraszko,<sup>19</sup> who observed a slight change in the thermal expansion coefficients at this temperature, and by Luspín et al., who noted a small change in elastic constants.<sup>8</sup> Baranowski and co-workers<sup>20</sup> observed a subtle transition, not at 149 °C, as most other groups have reported, but rather at 107 °C. What is quite clear from their work is that the thermal behavior of  $\text{CsH}_2\text{PO}_4$  in this lower temperature regime is highly dependent on sample state and environment, that is, whether the material is subjected to mechanical grinding or has been freshly prepared, and whether the atmosphere is humid or dry. Moreover, in no case have these transitions at 107 and 149 °C been found to be reversible, nor are they associated with superprotonic conductivity. Given that the presence or absence of these transitions is not relevant to the question of whether a superprotonic phase can exist in a compound such as  $\text{CsH}_2\text{PO}_4$ , with its particular hydrogen bond network, a detailed understanding of the behavior of  $\text{CsH}_2\text{PO}_4$  in this lower temperature regime is not the focus of the present work.

## Experimental Section

**Synthesis.** Powders of  $\text{CsH}_2\text{PO}_4$  were prepared by combining the starting reagents  $\text{Cs}_2\text{CO}_3$  (Alfa Aesar, 99.9%) and  $\text{H}_3\text{PO}_4$  (ACS, 85% w/w aqueous solution) in a molar ratio of 1:2 in aqueous solution. Rapid precipitation of  $\text{CsH}_2\text{PO}_4$  was induced by the introduction of methanol to the solution, and the resultant solids were then filtered from the mother solution. Single crystals of  $\text{CsH}_2\text{PO}_4$  were grown by slow evaporation of  $\text{H}_2\text{O}$  under ambient conditions from an aqueous solution into which this  $\text{CsH}_2\text{PO}_4$  powder had been dissolved. Confirmation that the desired material had been obtained was carried out by X-ray diffraction, using either a Siemens D 500 powder diffractometer (Cu  $K\alpha$  radiation) or a Syntex P21 4-circle, single-crystal diffractometer (Mo  $K\alpha$  radiation), as appropriate. Samples used in high-pressure experiments were first grown as single crystals, typically  $4 \times 4 \times 3$  mm<sup>3</sup> in volume, and then dried at  $\sim 100$  °C for 24 h prior to electrical characterization in order to minimize the influence of surface-adsorbed water.

**Ambient Pressure Characterization.** Thermal analysis was performed using a Netzsch STA 449C thermal analyzer, capable of simultaneous differential scanning calorimetry (DSC) and thermal gravimetry (TG), while  $\text{H}_2\text{O}$  off-gas (m 18.00) was recorded with a Pfeiffer Vacuum Thermal Star mass spectrometer. To quantify the extent to which the high-temperature properties of  $\text{CsH}_2\text{PO}_4$  are dependent upon surface area, thermal analysis was carried out on fine powders,

(16) Bronowska, W. *Adv. X-Ray Anal.* **1998**, *40*.

(17) Bronowska, W. *J. Chem. Phys.* **2001**, *114*, 611.

(18) Rapoport, E.; Clark, J. B.; Richter, P. W. *J. Solid State Chem.* **1978**, *24*, 423.

(19) Bronowska, W.; Pietraszko, A. *Solid State Commun.* **1990**, *76*, 293.

(20) Baranowski, B.; Friesel, M.; Lundén, A. *Z. Naturforsch.* **1986**, *41a*, 981.

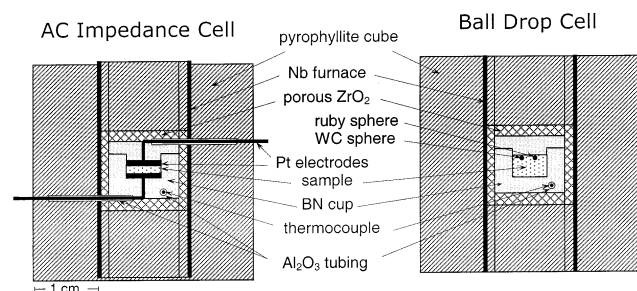


**Figure 3.** Cross-sectional schematic view of a high-pressure cell assembly used for (a) AC impedance measurements, and (b) ball drop experiment.<sup>21,22</sup>

coarse powders, and single-crystal pieces. Samples were prepared by milling large crystals which were then sieved into particle size ranges of 0–50  $\mu\text{m}$  (fine powder), 400–800  $\mu\text{m}$  (course powder), and 1 mm or greater (single crystals). Furthermore, several heating rates in the range of 0.5 to 25  $^{\circ}\text{C}/\text{min}$  were employed so as to enable extrapolation of results to zero heating rate or equilibrium behavior, as described below. The sample quantity was held constant at 5 mg for all experiments, and the atmosphere used was flowing  $\text{N}_2$  ( $\sim 40 \text{ cm}^3/\text{min}$ ).

Direct observations of the thermal behavior of  $\text{CsH}_2\text{PO}_4$  were made by optical microscopy. Single crystals were placed on a thermal stage in a transmission optical microscope, Leica DM LB, under polarized light and ambient atmospheres, and then heated. The thermal stage was heated to a maximum temperature of  $\sim 250 \text{ }^{\circ}\text{C}$ , a temperature not representative of the actual sample temperature.

The conductivity of  $\text{CsH}_2\text{PO}_4$  was measured by alternating current (AC) impedance spectroscopy using an HP 4284A Precision LCR Meter, a frequency range of 20 Hz to 1 MHz, and an applied voltage of 1.0 V under flowing dry nitrogen atmosphere. Both single crystal samples, approximately  $5 \times 5 \times 1 \text{ mm}$ , and polycrystalline pellets, uniaxially pressed at 100 psi to 1 cm in diameter and 1 mm in thickness, were examined. Ted Pella silver paint served as the electrode material. Impedance spectra were analyzed using the commercially available software package, ZView (Scribner & Assoc.).

Upon carrying out conductivity measurements, it became apparent that single crystal and polycrystalline samples behaved differently. To assess the source of this difference,  $^1\text{H}$  NMR was carried out on two types of samples. The first was a powder prepared by methanol-induced precipitation and dried at  $200 \text{ }^{\circ}\text{C}$  for 24 h prior to measurement, and the second was a powder obtained by grinding single crystals and immediately measured. Experiments were performed using a Bruker DSX 500 (11.7 T) at a spectral frequency of 500.2 MHz and a sample spin rate of 12 kHz.

**Conductivity at High Pressure.** High-pressure, high-temperature conductivity measurements were performed from room temperature to  $375 \text{ }^{\circ}\text{C}$  at  $1.0 \pm 0.2 \text{ GPa}$  upon several heating and cooling cycles. Single crystals were lightly ground and subsequently packed into a boron nitride (BN) cup with platinum electrodes on top and bottom. The cup was then placed into an AC impedance high-pressure cell, a schematic of which is shown in Figure 3(a). The pressure cell assembly was in turn loaded into a large-volume 1000-ton cubic anvil hydraulic press (H. T. Hall Inc.). In such a design, quasi-hydrostatic pressure is maintained by 12 gaskets formed by extrusion of the oversized pyrophyllite cube along its edges. Details of the experimental apparatus and pressure calibration are given elsewhere.<sup>21,22</sup> Each anvil, in electrical isolation from the other, makes contact through the faces of the cube with the Pt electrodes, Pt/Pt10%Rh thermocouple, and Nb foil

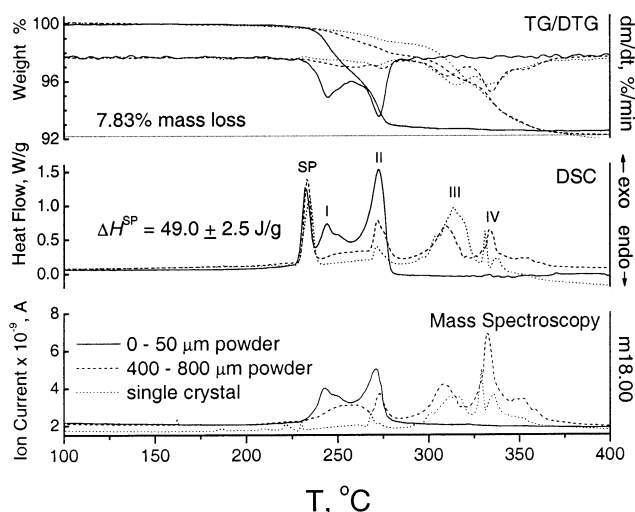


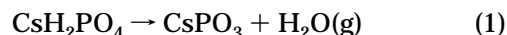
**Figure 4.** Results of simultaneous TG (top), DSC (middle), and mass spectroscopy (bottom) analysis for fine powder, coarse powder, and single crystals of  $\text{CsH}_2\text{PO}_4$ . Differential thermal gravimetric (DTG) data are also shown in top panel.

heater. A pressure–temperature correction was applied to the readings obtained from the Pt/Pt10%Rh thermocouple.<sup>23</sup> AC impedance data were collected using a Solartron SI 1260 impedance/gain-phase analyzer over the frequency range 10 Hz to 1 MHz and with an applied voltage of 1.0 V. Data analysis was again performed using the commercial software package, ZView (Scribner & Associates).

Because the sample cannot be directly observed in the high-pressure cell, one must establish whether measured changes in conductivity are due to melting of the sample or to a true solid–solid transition. To achieve this, a ball-drop experiment was performed. A 0.5-mm diam. ruby sphere and a 0.6-mm diam. tungsten carbide (WC) sphere, with 1 atm/22  $^{\circ}\text{C}$  densities of  $4.0 \text{ g cm}^{-3}$  and  $14.9 \text{ g cm}^{-3}$ , respectively, were placed on top of a powder sample packed into a BN cup, as shown in the schematic in Figure 3(b). The pressure cell was loaded into the same large-volume press utilized for AC impedance measurements, the pressure and temperature were raised to  $1.0 \pm 0.2 \text{ GPa}$  and  $325 \text{ }^{\circ}\text{C}$ , respectively, and the cell was held under these conditions for 10 min. Observation that the ruby and WC spheres remained suspended over the sample indicated that melting did not occur.

## Results and Discussion

**Thermal Analysis.** Typical thermal analysis results for  $\text{CsH}_2\text{PO}_4$  samples of different particle sizes and fixed heating rate ( $5 \text{ }^{\circ}\text{C}/\text{min}$ ) are presented in Figure 4. The thermal gravimetry (TG) and derivative thermal gravimetry (DTG) are shown in the top panel, differential scanning calorimetry (DSC) is shown in the middle panel, and mass spectroscopy measurements of  $\text{H}_2\text{O}$  (m 18.00) in the evolved gases are presented in the bottom panel. From the dehydration reaction



a weight loss of 7.83% is expected, and this value is noted in the top figure. It is evident from these thermal measurements that surface area plays a significant role in the decomposition/dehydration of  $\text{CsH}_2\text{PO}_4$  and may well explain the literature discrepancies noted above. For example, a weight loss of 7% was observed at  $278 \text{ }^{\circ}\text{C}$  for the fine powder, whereas for single crystals the

(21) Secco, R. A. *Can. J. Phys.* **1995**, *73*, 287.

(22) Secco, R. A. In *High-Pressure Science and Technology*; Schmidt, S. C., Shaner, J. W., Samara, G. A., Ross, M., Eds.; AIP Press: New York, 1993.

(23) Bundy, F. P. *J. Appl. Phys.* **1961**, *32*, 483.

same weight loss was not observed until 352 °C. Quite significantly, regardless of sample surface area, in all cases a polymorphic transition independent of decomposition is clearly evident at ~230 °C. Although the impact of this transition on conductivity cannot be assessed from thermal analysis alone, we identify this transformation as the superprotonic transition described earlier by Baranov et al.<sup>3</sup> At temperatures just beyond this structural transformation, dehydration occurs via multiple steps. The superprotonic phase transition (SP) and what are defined here as the first (I), second (II), third (III), and fourth (IV) dehydration processes are indicated in the figure. For fine powders only dehydration processes I and II were observed, whereas the coarse powder and single crystals exhibited only slight or no dehydration at I and II, with the majority of dehydration taking place at high-temperature processes III and IV.

The coincidence of the superprotonic phase transition with dehydration presents a challenge for the accurate measurements of the enthalpy  $\Delta H^{\text{SP}}$  of the superprotonic phase transition. To address this challenge, the enthalpy of the transition was evaluated only from single crystals in which dehydration processes I and II are minimized. A value of  $49.0 \pm 2.5$  J/g was obtained for a heating rate of 5 °C/min.

An inherent thermal lag in the thermal analysis can lead to systematic errors in true and measured transition and reaction temperatures as a function of heating rate. The difference ( $\Delta T$ ) between the temperature of the measured peak  $T_{\text{peak}}$  and the equilibrium onset temperature  $T_0$  of a transition or reaction of a pure compound is proportional to the heating rate  $V$ , sample mass  $m$ , transition enthalpy  $\Delta H$ , and the thermal resistance  $R$  as follows:<sup>24</sup>

$$\Delta T = (2m\Delta HRV)^{1/2} \quad (2)$$

Assuming a constant  $R$  and utilizing samples of equal mass, there should be a linear relationship between  $\Delta T$  and  $V^{1/2}$ . As  $V \rightarrow 0$ ,  $\Delta T \rightarrow 0$ , implying  $T_{\text{peak}} \rightarrow T_0$ . Therefore, by carrying out thermal analysis at several different heating rates and extrapolating to a heating rate of zero, one can estimate the "true" onset temperature for any thermal event.

As an example of the heating-rate dependent thermal behavior of  $\text{CsH}_2\text{PO}_4$ , a plot of the TG and DSC traces obtained at several different heating rates from a fine powder of  $\text{CsH}_2\text{PO}_4$  is shown in Figure 5. Analogous results were obtained for the coarse powder and single-crystal samples. The  $T_{\text{peak}}$  values for each process, as measured by DSC, DTG, and mass spectroscopy, are plotted as a function of  $V^{1/2}$  for fine powders in Figure 6. The results obtained from these three methods are in good agreement. Moreover, a linear relationship between  $T_{\text{peak}}$  and  $V^{1/2}$  is indeed evident. The true or equilibrium onset temperatures,  $T_0$ , determined by extrapolation to zero heating rate for each process and for each of the three sample types are summarized in Table 1. As is apparent from these data, whereas  $T^{\text{SP}}$  is relatively independent of surface area, the temperatures of the dehydration processes,  $T^{\text{I}} - T^{\text{IV}}$ , are not. Thus, for crystals of  $\text{CsH}_2\text{PO}_4$  heated rapidly, the

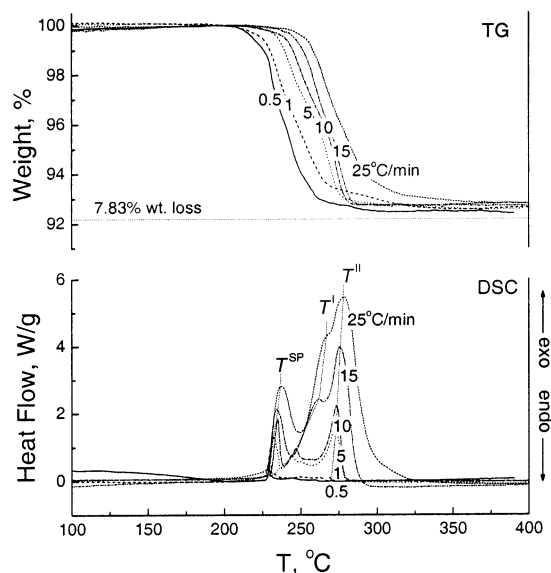


**Figure 5.** Results of simultaneous TG (top) and DSC (bottom) thermal analysis carried out at heating rates of 0.5, 1, 5, 10, 15, and 25 °C/min for fine powders of  $\text{CsH}_2\text{PO}_4$ .

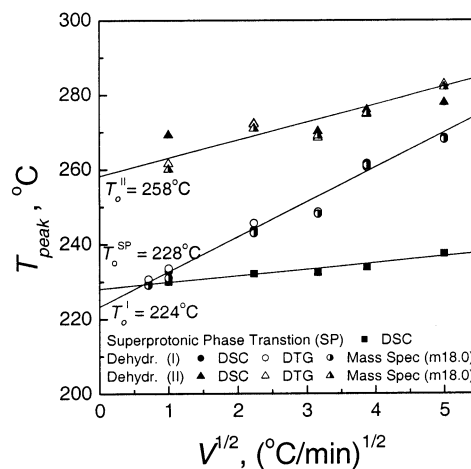


**Figure 6.** Superprotonic phase transition, and first and second dehydration process temperatures as a function of heating rate as measured by DSC, DTG, and mass spectroscopy for fine powders of  $\text{CsH}_2\text{PO}_4$ .

**Table 1. Onset Temperature of the Superprotonic Phase Transition ( $T_0^{\text{SP}}$ ), and of the First ( $T_0^{\text{I}}$ ), Second ( $T_0^{\text{II}}$ ), Third ( $T_0^{\text{III}}$ ), and Fourth ( $T_0^{\text{IV}}$ ) Decomposition Processes (Number in Parentheses Indicates the Uncertainty in the Final Digit)**

	$T_0^{\text{SP}}$	$T_0^{\text{I}}$	$T_0^{\text{II}}$	$T_0^{\text{III}}$	$T_0^{\text{IV}}$ (°C)
fine powder	228 (2)	224 (3)	258 (5)		
coarse powder	228 (2)	230 (4)	261 (4)	292 (5)	311 (10)
single crystals	228 (2)	230 (5)	261 (6)	298 (8)	325 (12)

superprotonic phase transition will likely be observed before dehydration; however, if sufficiently slow heating rates ( $<0.3$  °C/min) and large surface area powders are utilized, dehydration may precede the superprotonic transition.

**Optical Microscopy.** The optical microscopy studies support the conclusion that single-crystal  $\text{CsH}_2\text{PO}_4$  undergoes a structural transition prior to decomposition. Typical images obtained under cross-polarizers are shown in Figure 7. This particular crystal was approximately 0.5 mm on edge. At room temperature (prior to heating), the optically anisotropic, monoclinic

(24) Illers, K. *Eur. Polym. J.* **1974**, *10*, 911.

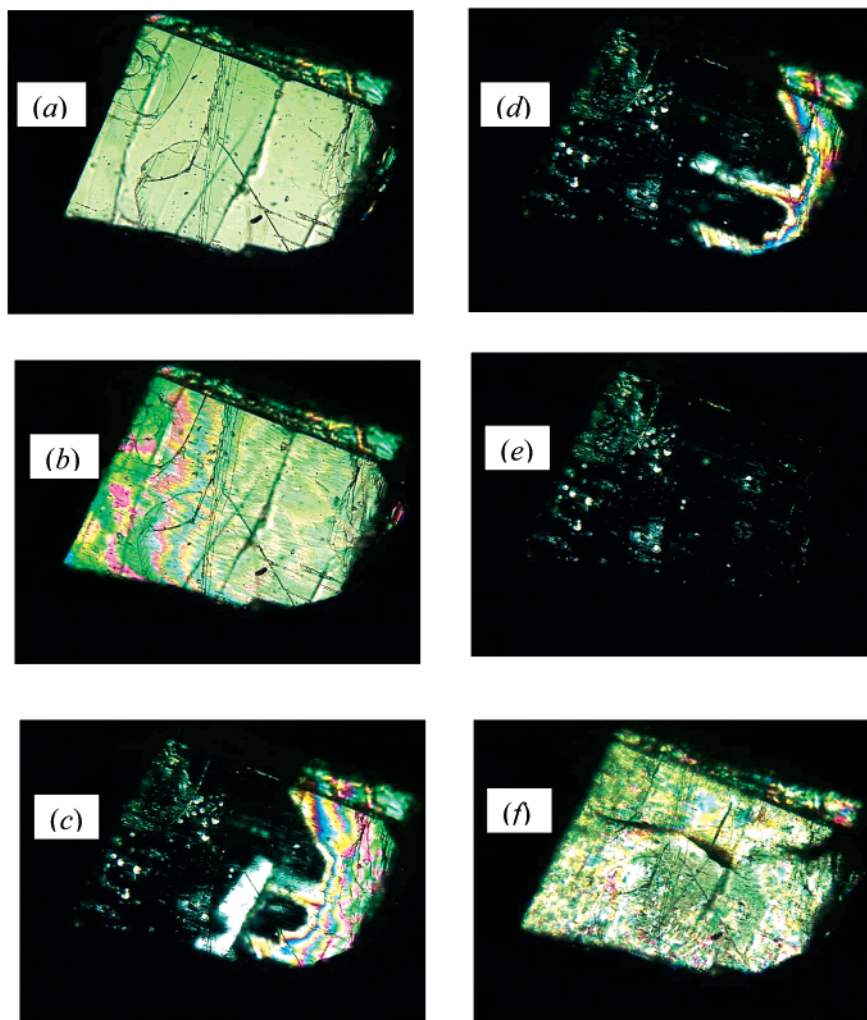


**Figure 7.** Polarized light microscopy images of a single crystal ( $\sim 0.5$  mm) of  $\text{CsH}_2\text{PO}_4$ : (a) at room temperature; (b) upon heating to  $250$  °C; (c,d,e) at  $250$  °C; and (f) after cooling back to room temperature.

form of  $\text{CsH}_2\text{PO}_4$  was observed, Figure 7(a). Upon heating to  $\sim 250$  °C, a rainbow-colored phase-front traveled from left to right across the crystal, leaving behind a new phase which was optically isotropic (black) and presumably cubic, Figure 7(b) through (e). Upon cooling to room temperature, the crystal transformed back to an optically anisotropic phase, Figure 7(e) and (f), with some evidence of slight damage to the crystal quality. The reversible nature of this observed transformation is strong evidence for a polymorphic phase transition as opposed to decomposition.

**Conductivity at Ambient Pressure.** The results of the conductivity measurements for both single crystal and polycrystalline samples under ambient pressure conditions are shown in Figure 8 in Arrhenius form. The corresponding Nyquist plots [ $Z_{\text{real}}$  (or  $Z'$ ) vs  $-Z_{\text{imag}}$  (or  $-Z''$ ) as parametric functions of frequency] obtained at temperatures above  $T^{\text{SP}}$  are presented in Figure 9. The conductivity of both sample types increased sharply at the transition temperature, however, in neither case to the high value reported by Baranov et al.<sup>3</sup> Moreover the jump in conductivity was significantly lower for the polycrystalline pellet than for the single-crystal sample. Beyond  $T^{\text{SP}}$  neither sample type exhibited a linear, Arrhenius region, as is typical for other superprotonic conductors. The polycrystalline pellet exhibited a monotonic decrease in conductivity, also evident in Figure

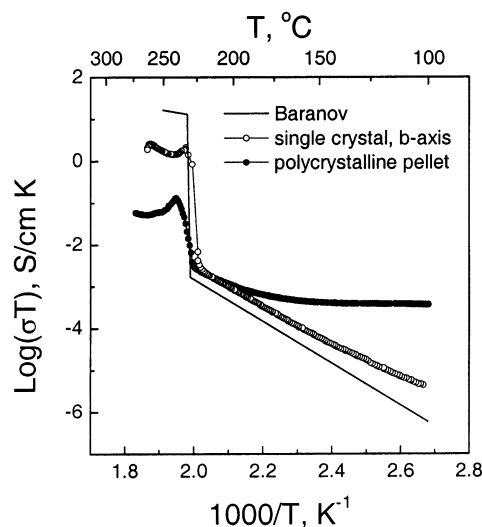


**Figure 8.** Arrhenius plot of the conductivity upon heating a  $\text{CsH}_2\text{PO}_4$  crystal and polycrystalline pellet, and compared to the results of Baranov et al.<sup>3</sup>

9(b), whereas the single crystal sample exhibited more erratic behavior, although the conductivity generally increased from  $245$  to  $260$  °C, Figure 9(a). As might be expected, the high-temperature behavior of  $\text{CsH}_2\text{PO}_4$  was highly sample-dependent, with polycrystalline

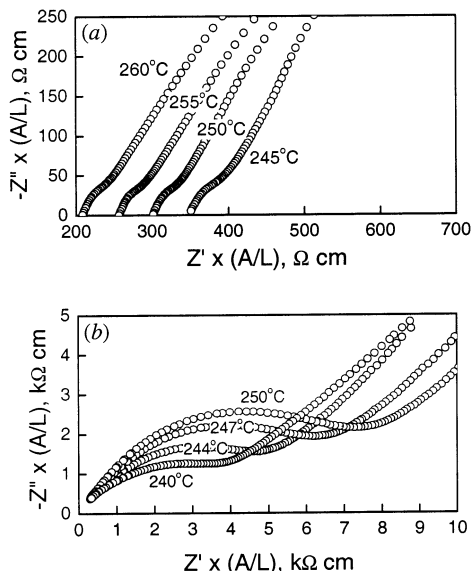


**Figure 9.** Nyquist plots at various temperatures of  $\text{CsH}_2\text{PO}_4$  upon heating above  $T^{\text{SP}}$  for (a) a crystal and (b) a polycrystalline pellet.

samples and small single crystals typically exhibiting lower conductivity and lower stability above  $T^{\text{SP}}$  than large single crystals. These results are consistent with those of previous investigations in which the electrical behavior of the superprotonic phase could be observed, such as by Baranov et al.,<sup>3</sup> for sufficiently large crystals, whereas for smaller crystals, dehydration prevented such observations.<sup>4</sup> In almost every case, samples measured upon cooling, either single crystals or polycrystalline pellets, did not exhibit conductivities as high as that obtained upon heating (not shown), indicating that the sample had undergone some degree of decomposition at elevated temperatures.

At temperatures below  $T^{\text{SP}}$ , a large difference between the conductivities of the single crystal (*b*-axis oriented) and polycrystalline samples is evident, Figure 8. Furthermore, both appear more conductive than the  $\text{CsH}_2\text{PO}_4$  reported by Baranov et al.<sup>3</sup> Fitting the conductivity,  $\sigma$ , of the  $\text{CsH}_2\text{PO}_4$  single crystal to the Arrhenius law

$$\sigma(T) = \frac{A}{T} \exp\left(\frac{-\Delta H_a}{k_B T}\right) \quad (3)$$

where  $A$  is a preexponential factor,  $T$  is temperature,  $k_B$  is the Boltzmann constant, and  $\Delta H_a$  is the activation enthalpy, yields values for  $A$  and  $\Delta H_a$  of  $4.0 \times 10^6$  (2)  $\Omega^{-1}\text{-cm}^{-1}\text{K}$  and 0.91 (4) eV, respectively. Values of  $A$  and  $\Delta H_a$  for the polycrystalline samples are not reported here as they were highly dependent on sample history. Specifically, upon drying for long periods the conductivity of polycrystalline pellets gradually decreased. The apparent discrepancy between the conductivities of the single crystal and polycrystalline samples of  $\text{CsH}_2\text{PO}_4$  was further investigated by measuring the conductivity of a polycrystalline pellet as a function of time at 200 °C under flowing dry nitrogen. The pellet was prepared from powders obtained by methanol-induced precipitation. The impedance data initially showed a single arc in the Nyquist representation, but after approximately 24 h a second low-frequency arc became evident, Figure

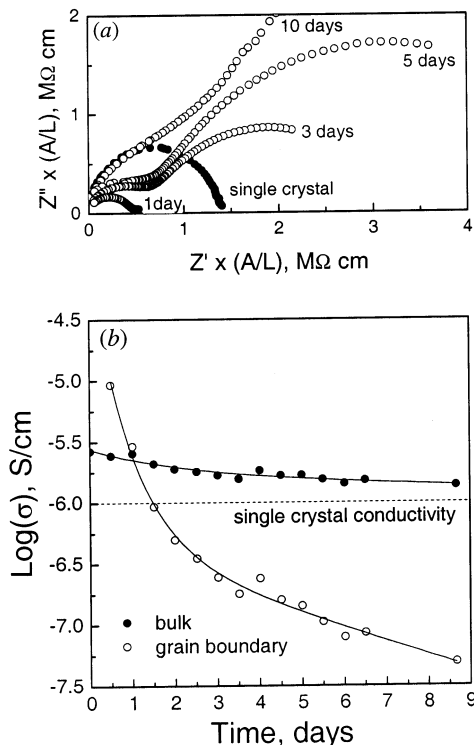


**Figure 10.** AC impedance of polycrystalline  $\text{CsH}_2\text{PO}_4$  held at 200 °C: (a) Nyquist plots obtained at various times, with single-crystal results shown for comparison; and (b) bulk and grain boundary conductivity as a function of time; the conductivity of a single crystal is as indicated.

10(a). This low-frequency arc was attributed to grain boundary conductivity, and the high-frequency arc to bulk conductivity. With increasing time, both the grain boundary and bulk conductivities decreased and the bulk conductivity approached that of single-crystal  $\text{CsH}_2\text{PO}_4$ , Figure 10(b). These results suggest that the apparently high conductivity measured in polycrystalline samples is due to chemisorbed  $\text{H}_2\text{O}$ , which is very gradually desorbed at elevated temperatures. Materials such as  $\text{Zr}(\text{HPO}_4)_2$ , in both hydrated and anhydrous form, are known to show a somewhat similar humidity dependence in their transport behavior due to adsorbed water between the layers of the highly layered crystal structure.<sup>25</sup> However, retention of water at such high temperatures and for such long periods, as observed here, is unusual for a crystalline acid phosphate. Finally, we note that in this analysis, the grain boundary conductivity has not been normalized to account for the grain boundary density, as would be necessary to compare samples with different grain sizes.<sup>26</sup>

**NMR Spectroscopy.** The proton NMR spectra of two  $\text{CsH}_2\text{PO}_4$  powders, the first produced by methanol-induced precipitation and the second by grinding a single crystal, are presented in Figure 11. As stated above, the methanol-precipitated powder was dried at 200 °C for 24 h prior to measurement, whereas the ground single crystal was examined immediately after the grinding step. For both powders, peaks were observed at 14.5 and 10.9 ppm, which correspond to the

(25) Alberti, G.; Casciola, M.; Costantino, U.; Radi, R. *Gazz. Chim. Ital.* **1979**, *109*, 421.

(26) Haile, S. M.; West, D. L.; Campbell, J. *J. Mater. Res.* **1998**, *13*, 1576.

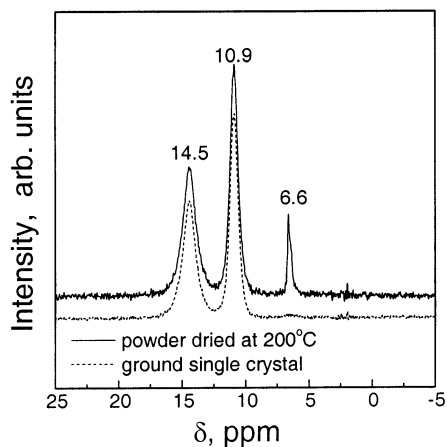


**Figure 11.** Solid-state  $^1\text{H}$  NMR spectra of  $\text{CsH}_2\text{PO}_4$  powders obtained by (i) methanol induced precipitation and then dried for 24-hours at  $200^\circ\text{C}$  prior to measurement; and (ii) from ground single crystals.

two crystallographically distinct hydrogen atoms observed in the room-temperature structure of  $\text{CsH}_2\text{PO}_4$ .<sup>27</sup> However, for the methanol-precipitated powder an additional peak was observed at 6.6 ppm. On the basis of extensive studies of chemically similar calcium phosphates, in which chemical shifts of 5.5–6.2 ppm were observed for surface-adsorbed water,<sup>28</sup> we conclude that this third peak corresponds to chemically surface-adsorbed water. It is thus evident that chemisorbed surface water is particularly difficult to remove from  $\text{CsH}_2\text{PO}_4$ , and that this water affects not only grain boundary conductivity, but also the impedance arc normally associated with bulk conductivity behavior. It is for this reason that well-dried single crystals were used (in crushed form) in the high-pressure conductivity experiments.

**Conductivity at High Pressure: Results.** The pressure–temperature conditions employed in the present experiments can be compared to the phase diagram reported by Rapoport et al.,<sup>18</sup> schematically reproduced in Figure 12. The dashed horizontal line at  $149^\circ\text{C}$  in this figure refers to a quasi-irreversible phase transition noted by those authors, from the room-temperature phase III to an unidentified phase II. The results of the conductivity measurements, which would be expected to traverse both the III/II and II/I transitions, are presented in Figure 13. Upon heating for a first time, a sharp increase in conductivity was first observed at  $150^\circ\text{C}$ . In response to further heating, a second sharp increase in conductivity occurred at  $260^\circ\text{C}$ , beyond which Arrhenius behavior was exhibited up to  $375^\circ\text{C}$ . Upon cooling, the high-temperature transition exhibited a large hysteresis, with the conductivity dropping by several orders of magnitude at about  $240^\circ\text{C}$ . A second heating revealed no anomalous behavior at  $150^\circ\text{C}$ , indicating the irreversible nature of this feature, consistent with earlier studies.<sup>18</sup> Upon further heating, the superprotonic transition at  $260^\circ\text{C}$  was reproduced. While cooling in this second thermal cycle, a large hysteresis was again observed with a reverse transition at about  $240^\circ\text{C}$ . In general, the magnitude

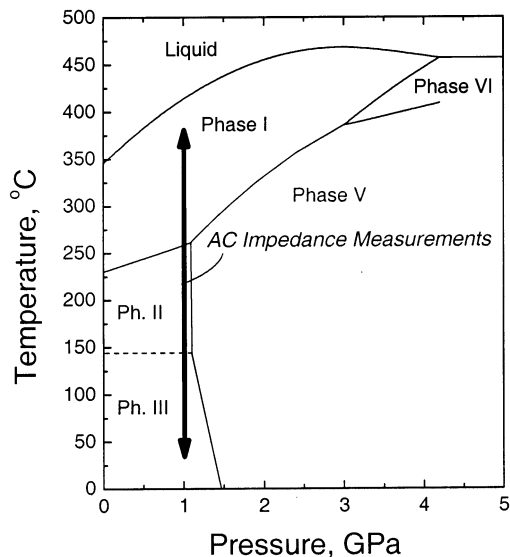


**Figure 12.** Pressure–temperature phase diagram of  $\text{CsH}_2\text{PO}_4$  from Rapoport et al.<sup>18</sup> showing the path over which AC impedance measurements were carried out in this work.

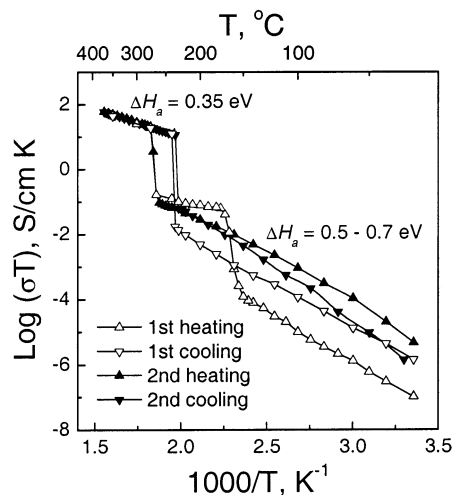


**Figure 13.** Conductivity of polycrystalline  $\text{CsH}_2\text{PO}_4$  obtained at 1 GPa upon two heating and cooling cycles, and plotted in Arrhenius form. The activation enthalpy for charge transport ( $\Delta H_a$ ) is indicated for the superprotonic phase ( $260$ – $375^\circ\text{C}$ ) and for the stable, low-temperature phase ( $25$ – $260^\circ\text{C}$ ).

of the conductivity at high temperature was highly reproducible upon multiple heating and cooling cycles, whereas that at low temperature ( $25$  to  $260^\circ\text{C}$ ) was not.

Representative Nyquist plots of the measured AC impedance spectra above and below the superprotonic phase transition are presented in Figure 14. Below the transition, Figure 14(a), the intercept of the semicircle with the real axis ( $Z'$ ) is interpreted as the resistivity of the sample; whereas above the transition, Figure 14(b), the intercept of the electrode response with  $Z'$  is taken as the sample's resistivity. In both cases, the resistivity decreases with increasing temperature. This result differs from the ambient pressure behavior, Figure 8, for which the resistivity of the sample increased with increasing temperature above the transition. With these data, we conclude that the observed high-temperature electrical behavior while under pressure is due to the superprotonic phase of  $\text{CsH}_2\text{PO}_4$ ,

(27) Nelmes, R. J.; Choudhary, R. N. P. *Solid State Commun.* **1978**, *26*, 823.

(28) Yesinowski, J.; Eckert, H. *J. Am. Chem. Soc.* **1987**, *109*, 1274.



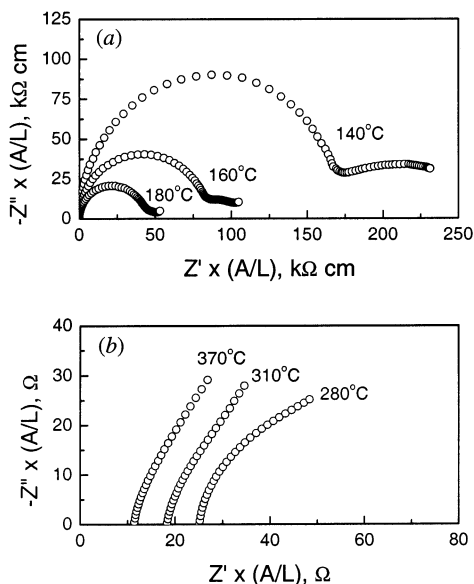


**Figure 14.** Nyquist representation of impedance data obtained from polycrystalline CsH<sub>2</sub>PO<sub>4</sub> at 1 GPa (a) below and (b) above the superprotonic phase transition.

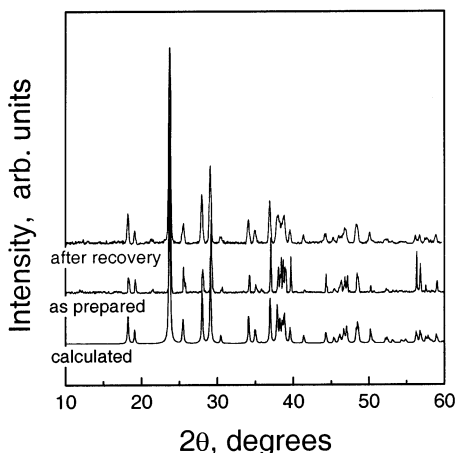


**Figure 15.** X-ray powder diffraction patterns of CsH<sub>2</sub>PO<sub>4</sub>: calculated,<sup>2</sup> as prepared, and after recovery from 350 °C and 1 GPa; backgrounds subtracted from experimental patterns.

whereas at atmospheric pressure the electrical behavior is complicated by dehydration processes.

Powder X-ray diffraction data collected from CsH<sub>2</sub>PO<sub>4</sub> under ambient conditions after heating to 350 °C at 1 GPa, showed that the transformations undergone by CsH<sub>2</sub>PO<sub>4</sub> under high-temperature, high-pressure conditions are reversible. Figure 15 shows the calculated X-ray powder diffraction pattern for the *P*2<sub>1</sub>/*m* paraelectric phase of CsH<sub>2</sub>PO<sub>4</sub><sup>2</sup> along with those of the experimental diffraction patterns of samples “as prepared” and “after recovery” from the high temperature, high-pressure conditions. The similarity of the patterns demonstrates that the material did not undergo any kind of (irreversible) decomposition. Together with the results of the ball drop experiments described above, these data confirm that all of the effects evident in Figure 13 are due to solid–solid transformations.

**Conductivity at High Pressure: Discussion.** The high-temperature phase encountered in this work clearly corresponds to that identified as “Phase I” by Rapoport

et al.<sup>18</sup> Those authors reported a transition to this phase at 258 °C under 1 GPa pressure, comparable to the transition temperature of 260 °C measured here. The dramatic increase in conductivity at the transition, along with the low activation enthalpy for proton transport (see below), indicates Phase I is “superprotonic” in nature. These results thus support the findings of Baranov et al. that CsH<sub>2</sub>PO<sub>4</sub> undergoes a solid–solid transformation that leads to high conductivity, independent of decomposition.<sup>3</sup> It can be further concluded that this superprotonic phase corresponds to the cubic *Pm*3̄*m* phase reported by Preisinger et al. above 230 °C at atmospheric pressure.<sup>7</sup> From their diffraction studies, Preisinger and co-workers reported a change in volume ( $\Delta V$ ) at the superprotonic transition of 3.6 Å<sup>3</sup>. Using the Clapeyron equation, this value of  $\Delta V$ , along with a  $\Delta S$  of 30 J mol<sup>-1</sup> K<sup>-1</sup>,<sup>4</sup> we would expect a transition that occurs at ~ 300 °C at 1 GPa, slightly higher than that observed in this work.

In the present study, an irreversible anomaly at ~150 °C was observed at 1 GPa upon an initial heating. The nature of this apparent transition and the phase to which CsH<sub>2</sub>PO<sub>4</sub> transforms at this temperature, Phase II, remain unclear; no signature of this phase was observed at ambient pressures. As stated above, there is significant ambiguity concerning this apparent transition, with researchers reporting transition temperatures ranging from 107 to 149 °C at ambient pressure, and 149 to 167 °C at 1 GPa,<sup>29</sup> depending on the details of the sample preparation. Resolving these ambiguities is beyond the scope of the present study.

Fitting the conductivity,  $\sigma$ , of superprotonic CsH<sub>2</sub>PO<sub>4</sub> to the Arrhenius law, eq 3, yields values for *A* and  $\Delta H_a$  of  $3.2 \times 10^4 \text{ } \Omega^{-1}\text{-cm}^{-1}\text{K}$  and 0.35 eV, respectively. In comparison, the values reported by Baranov et al.<sup>3</sup> for superprotonic, single-crystal CsH<sub>2</sub>PO<sub>4</sub> at ambient pressure are  $A = 2 \times 10^4 \text{ } \Omega^{-1}\text{-cm}^{-1}\text{K}$  and  $\Delta H_a = 0.32 \text{ eV}$ . The difference between the two activation enthalpies indicates that pressure increases the barrier to proton transport. This increase in  $\Delta H_a$  can be quantified in terms of the activation volume for proton conduction using the relationship

$$\Delta H_a = \Delta E_a + P\Delta V_a \quad (4)$$

where *P* is pressure and  $\Delta E_a$  and  $\Delta V_a$  are the activation energy and volume, respectively. The result,  $\Delta V_a = 2\text{--}3 \text{ cm}^3/\text{mol}$ , corresponds to 3–4% of the unit cell volume. This value is comparable to those determined from high-pressure studies of other superprotonic solid acids, such as CsHSO<sub>4</sub>, Rb<sub>3</sub>H(SeO<sub>4</sub>)<sub>2</sub>, and (NH<sub>4</sub>)<sub>3</sub>H(SO<sub>4</sub>)<sub>2</sub>.<sup>30,31</sup> It is noteworthy, however, that in some cases, for example CsHSO<sub>4</sub> in its low-temperature phase,<sup>32</sup> the activation volume for proton conduction can be negative, reflecting the unique transport mechanism for this species as compared to other ions for which steric hindrances to motion are dominant.

(29) Baranowski, B.; Friesel, M.; Lundén, A. *Phys. Scripta* **1988**, *37*, 209.

(30) Dilanyan, R. A.; Sinitsyn, V. V.; Shekhtman, V. Sh.; Baranov, A. I.; Shuvalov, L. A. *Crystallogr. Rep.* **1994**, *39*, 428.

(31) Sinitsyn, V. V.; Baranov, A. I.; Ponyatovsky, E. G.; Shuvalov, L. A. *Solid State Ionics* **1995**, *77*, 118.

(32) Sinitsyn, V. V.; Ponyatovsky, E. G.; Baranov, A. I.; Tregubchenko, A. V.; Shuvalov, L. A. *Sov. Phys. JETP* **1991**, *73*, 386.

### Conclusions

The results presented here demonstrate incontrovertibly that  $\text{CsH}_2\text{PO}_4$  undergoes a polymorphic phase transition at  $228 \pm 2$  °C under atmospheric pressures. Depending on the sample surface area, the transition can coincide with thermal decomposition, but reveals itself as an independent phase transition for large single-crystal samples and upon rapid heating. The enthalpy of this transition is  $49.0 \pm 2.5$  J/g. The conductivity of  $\text{CsH}_2\text{PO}_4$  rises sharply at the transition, however, the extent to which it increases is, again, highly sample dependent. Differences in thermal behavior due to differences in surface area and heating rates are likely the reason for significant literature discrepancies regarding this compound. Under ambient conditions, the high-temperature phase does not exhibit sufficient thermal stability for complete characterization, motivating high-pressure investigations. In addition, strongly bound surface water can play a significant role in the conductivity of  $\text{CsH}_2\text{PO}_4$ , particularly at temperatures below the transition. At a pressure of 1 GPa, the superprotonic transition occurs at 260 °C, and the high-temperature phase is stable over a rather wide temperature regime. Thus, high-pressure experiments may be ideal for examining the high-temperature behavior of other solid acids in which dehydration competes with polymorphic transitions at ambient pressure.

The existence of a superprotonic transition in  $\text{CsH}_2\text{PO}_4$  demonstrates that solid acids, in which all the oxygen atoms are hydrogen bonded at low temperature, can exhibit such transitions. The order–disorder model that is appropriate for describing the high-temperature phase of  $\text{CsHSO}_4$ ,<sup>10</sup> and presumably, also of  $\text{M}_3\text{H}(\text{XO}_4)_2$  compounds such as  $\text{Rb}_3\text{H}(\text{SeO}_4)_2$ ,<sup>33</sup> and which would have ruled out a transition in  $\text{CsH}_2\text{PO}_4$ , accordingly does not apply here. In those other materials, there is a close structural relationship between the superprotonic and ordered phases, whereas no such simple relationship appears to exist in  $\text{CsH}_2\text{PO}_4$ . The uniformity in the hydrogen bond network of  $\text{CsH}_2\text{PO}_4$ , may, however, be responsible, by reducing the entropic driving force for the transformation, for the limited temperature regime of stability of the superprotonic phase under ambient conditions.

**Acknowledgment.** This work was supported by a grant from the U.S. National Science Foundation. We thank Dr. Sonjong Hwang at Caltech's Solid State NMR Facility for assistance with NMR measurements.

CM020138B

---

(33) Pawlowski, A.; Pawlaczyk, Cz.; Hilczer, B. *Solid State Ionics* **1990**, *44*, 17.